Polymer Journal (2014) 46, 492–498

www.nature.com/pj

ORIGINAL ARTICLE

Near-infrared light-responsive shape-memory poly(ε-caprolactone) films that actuate in physiological temperature range

Qinghui Shou[1,2], Koichiro Uto[2], Masanobu Iwanaga[3], Mitsuhiro Ebara[2] and Takao Aoyagi[1,2]

Near-infrared (NIR) light-responsive shape-memory films were prepared through the photo-initiated polymerization of poly(ε-caprolactone) (PCL) macromonomers with acryloyl terminal groups in the presence of gold nanorods (AuNRs). To incorporate the AuNRs homogenously within the films, the surfaces of AuNRs were also modified with PCL via surface-initiated ring-opening polymerization. The shape-switching temperature of PCL was adjusted in the physiological temperature range by controlling the melting temperature of PCL. Exposure to NIR light successfully induced the photothermal heating of embedded AuNRs and, consequently, the shape-switching transition. After NIR irradiation at higher-power densities, the film completely recovered its original shape. When exposed to lower-power densities, a local temperature increase was observed in the area where the beam hit. Therefore, local shape memory transformations were obtained. These results show the potential of gold nanorod-embedded PCL films as spatially controllable, shape-memory materials that actuate in physiologically relevant temperature ranges and from remote stimuli.
Polymer Journal (2014) **46,** 492–498; doi:10.1038/pj.2014.48; published online 18 June 2014

Keywords: grafting from; gold nanorods; near-infrared light; poly(ε-caprolactone); photothermal effect; shape-memory

INTRODUCTION

Shape-memory polymers (SMPs), which have the ability to return from a deformed state to their original shape after receiving an external stimulus, have drawn much attention during fundamental research into practical applications.[1] SMPs possess several advantages compared with shape-memory alloys due to the large deformation ability, low cost, environmentally friendly processing, and potential biocompatibility and biodegradability. These advantages are especially significant for biomedical applications, such as minimally invasive implants.[1,2] Among the SMPs, thermally induced SMPs are the most extensively investigated group of SMPs.[3] They are thermoplastic elastomers or thermosets that are programmed by mechanically deforming the shape of a polymer at a temperature that exceeds its glass transition temperature (T_g) or melting temperature (T_m). This deformed shape (or temporary shape) can be fixed when the material is cooled below the T_g or T_m. If the polymer chains are chemically or physically cross-linked, the material returns to its original shape (or permanent shape) by heating it above the T_g or T_m. During this process, an increase in entropy serves as the driving force for the material to recover its initial shape. Therefore, the use of T_m as the triggering switch is more favorable because the enthalpy change of the solid–liquid phase transition is much larger than that of a glass–rubber transition.

We have been developing a thermally induced SMP switch with a T_m at a biologically relevant temperature using cross-linked poly(ε-caprolactone) (PCL).[4] PCL is an important biocompatible and biodegradable synthetic polymer and has been approved for biomedical applications by the US Food and Drug Administration.[5] Lendlein *et al.*[6] developed shape-memory biodegradable sutures using oligomeric PCL. Rodriguez *et al.*[7] reported miscible blends comprising linear PCL and chemically cross-linked PCL networks. The blends demonstrate unique shape-memory-assisted self-healing, which is the material's ability to close local microscopic cracks and heal those cracks by bonding between the cracked surfaces. Neuss *et al.*[8] developed shape-memory tissue-engineering scaffolds using a cross-linked PCL dimethacrylate network. We have recently demonstrated PCL cell culture surfaces with shape-memory nanopatterns.[4] The direction of the aligned cells on the nanopatterns can be turned to a perpendicular direction via the shape-memory activation of the nanopatterns that transition from a temporary pattern to the original, permanent pattern by heating to 37 °C.[9] We have also envisioned applications of this surface

[1]Graduate School of Pure and Applied Sciences, University of Tsukuba, Ibaraki, Japan; [2]Biomaterials Unit, Smart Biomaterials Group, International Center for Materials Nanoarchitectonics (WPI-MANA), National Institute for Materials Science (NIMS), Ibaraki, Japan and [3]Photonic Materials Unit, National Institute for Materials Science (NIMS), Ibaraki, Japan
Correspondence: Professor, Dr T Aoyagi, Biomaterials Unit, Smart Biomaterials Group, International Center for Materials Nanoarchitectonics (WPI-MANA), National Institute for Materials Science (NIMS), 1-1 Namiki, Tsukuba, Ibaraki 305-0044, Japan.
E-mail: aoyagi.takao@nims.go.jp
Received 2 March 2014; revised 17 April 2014; accepted 21 April 2014; published online 18 June 2014

shape-memory phenomenon in the areas of microfluidic control systems that actuate at biologically relevant temperatures, such as pumps and valves.[10]

Although thermal activation is advantageous because it allows penetration through materials, the local and remote activation of the shape-memory effect is appealing when considering biological applications. To achieve this goal, researchers have focused on the photothermal effect of metal nanoparticles or photochromic dyes.[11,12] The photothermal effect is a phenomenon produced by the photoexcitation of a material, resulting in the production of thermal energy.[13] Of these materials, gold nanoparticles have been widely employed in numerous biomedical applications, including hyperthermia therapy and biological sensing, due to their biocompatibility.[14,15] Cylindrical gold nanorods (AuNRs) have become a new and exciting target due to their biocompatibility, optical properties and photothermal effects.[16] One of the advantages is that the surface plasmon resonance (SPR) extinction of AuNRs in the near-infrared (NIR) region (650–900 nm) provides opportunities for NIR photoabsorption and scattering, in which region there is very limited absorption for most biological tissues, including hemoglobin and water.[17] There have been several reports on remote-controllable SMPs using AuNRs.[18,19] For example, Hribar *et al.*[18] recently reported on NIR light-induced temperature transitions in the shape-memory composites of biodegradable poly(β-amino ester)s and AuNRs. The heating can change the network from a glassy to a rubbery system (T_g: 44–53 °C) and change the polymer from a temporary shape to its permanent shape.

In the present work, NIR-responsive shape-memory films were developed through the photo-initiated polymerization of PCL macromonomers with acryloyl terminal groups in the presence of AuNRs. The surfaces of the AuNRs were also modified with PCL through surface-initiated ring-opening polymerization (SI-ROP) to incorporate the AuNRs homogenously within the films. The shape-memory-switching temperatures of the PCL films were successfully adjusted to near-body temperature while retaining a sharp transition over a narrow temperature range. Finally, the local and remote activation of shape-memory effects were demonstrated by irradiating with NIR light over a limited area.

EXPERIMENTAL PROCEDURE

Materials

Gold (III) chloride trihydrate, cetyltrimethyl ammonium bromide (CTAB), sodium borohydride ($NaBH_4$), silver nitrate, L-ascorbic acid and 2,2-dimethoxy-2-phenylacetophenone (DMPA) as a photo initiator, were purchased from Sigma-Aldrich (St Louis, MO, USA). 4-Mercaptophenol was purchased from Tokyo Chemical Industry (Tokyo, Japan). ε-Caprolactone was purchased from Tokyo Chemical Industry and purified by distillation over calcium hydride under reduced pressure. Tetrahydrofuran (THF), acetone, methanol and other organic solvents used in this work were purchased from Wako Pure Chemical Industries (Osaka, Japan). Milli-Q purified water (Merck, Millipore, MA, USA) was used in all experiments. Unless otherwise stated, all of the chemicals were used as received.

Measurements

Ultraviolet–visible–NIR absorption experiments were performed using a UV/Vis/NIR spectrophotometer (V-7200 Jasco, Tokyo, Japan). To measure the absorption of the samples, reflectance mode was utilized and transformed to absorption mode. Transmission electron microscopy (TEM) images were obtained on a JEM-2100F (JEOL, Tokyo, Japan). Phosphotungstic acid hydrate was used as the negative staining agent. The particle size distributions were obtained by measuring more than 50 particles from the corresponding transmission electron micrographs using SmileView software (JEOL, Tokyo, Japan). To prepare thin films for TEM observation, a xylene solution of PCL and PCL-modified AuNRs was prepared by vortex mixing and ultrasonication, and held for 2 h to form a homogenous solution. A TEM grid with a thin carbon film coating was fixed on the sample holder of a spin-coating machine. After that, 5 μl of the sample was dropped onto the copper TEM grid, and spin coating was immediately performed to disperse the liquid sample (speed: 8000 r.p.m.; acceleration time: 1 s; spin time: 60 s). ^{1}HNMR (300 MHz, JEOL, Tokyo, Japan) was used for the characterization of the polymers and nanorods. $CDCl_3$ was used as the solvent. To avoid peak broadening of the thiol-protected gold nanoparticles, iodine was used to cleave the Au–S covalent bond.[20] The melting temperature was measured using differential scanning calorimetry (DSC 6100, Seiko Instruments, Chiba, Japan) at a programming rate of 5 °C per min. The degree of crystallinity was calculated based on the equation $\chi = \frac{\Delta H_m}{\Delta H_m^0} \times 100\ \%$. ΔH_m is the melting enthalpy of the samples used in this work. ΔH_m^0 is the melting enthalpy of full crystalline PCL (139.5 J g^{-1}).[21] The successful surface grafting of PCL on the AuNRs was evaluated via weight loss during thermogravimetric analysis as a function of temperature (TGA, EXSTAR6000 TG/DTA, SII Nanotechnology, Tokyo, Japan). The surface temperatures of the samples were measured using an infrared camera (FLIR System Japan K.K., Tokyo, Japan).

Preparation of PCL-modified AuNRs via SI-ROP

First, AuNRs were synthesized using a seed-mediated growth method.[22,23] Briefly, spherical gold nanoparticles (3 nm) were used as the seeds, and CTAB was used as a capping agent to direct the anisotropic growth of the gold clusters to form cylindrical-shaped AuNRs. Then, hydroxyl groups were introduced to the surfaces of the AuNRs using the reported method.[23] Briefly, 4-mercaptophenol (2.5 g) in 30 ml of THF was added to the aqueous AuNRs solution. After 12 h, the 4-mercaptophenol-modified AuNRs were separated by rinsing with THF and by centrifugation several times. Finally, SI-ROP of ε-caprolactone was carried out using 4-mercaptophenol-modified AuNRs as an initiator. Briefly, AuNRs (10 mg) were placed in a round-bottom flask and dried under reduced pressure, and 20 ml of ε-caprolactone and a catalytic amount of tin hexanoate was then injected into the flask. The mixture was reacted at 60 °C for 24 h under a nitrogen atmosphere. After the SI-ROP reaction, 20 ml of THF was added to the above solution. After centrifugation at a speed of 3500 r.p.m., the precipitated AuNRs, which were not well modified by PCL, were removed, and the supernatant was poured into a large amount of diethyl ether and hexane (volume ratio = 1:1). The precipitate was rinsed several times with diethyl ether and hexane. Finally, the precipitate was dried under vacuum and stored in a desiccator.

Preparation of AuNR-embedded PCL films

The gold nanorod-embedded shape-memory PCL films were prepared by cross-linking two- and four-branched PCL (2b- and 4b-PCL) with acrylate end-groups in the presence of AuNRs. Briefly, 2b- and 4b-PCL were synthesized using a ring-opening polymerization that was initiated by tetramethyleneglycol and pentaerythritol, respectively.[4] Acryloyl chloride was then reacted with the ends of the branched chains. The average degrees of polymerization of each branch on the 2b- and 4b-PCL were 20 and 10, respectively. The obtained PCL macromonomers were dissolved in xylene containing DMPA (15 wt%) and PCL-modified AuNRs at varying concentrations. The solution was injected between glass slides with a 0.2-mm Teflon spacer. The PCL macromonomers were cured at 30 °C for 3 h under ultraviolet light irradiation (wavelength 365 nm, 2 mW cm^{-2}). In this study, four different films with 50/50 or 70/30 wt% of 2b-/4b-PCL and 0.3–0.4 or 2.4–2.5 wt% of AuNRs were prepared. They are abbreviated as 50/50 PCL-low, 50/50 PCL-high, 70/30 PCL-low and 70/30 PCL-high.

NIR light-responsive shape-recovery performance

The shape-memory performance was evaluated in the order listed below. First, the PCL film (3 mm by 1.2 cm) was heated to 40 °C (above T_m) and elongated to the predetermined strain of 100%, and the temperature was then cooled to 4 °C (below the crystallization temperature, T_c) for 10 min to fix the applied strain while maintaining the tensile strain. The films were then irradiated with 805 nm NIR at varying power densities between 0.4 and 1 W cm^{-2} at a

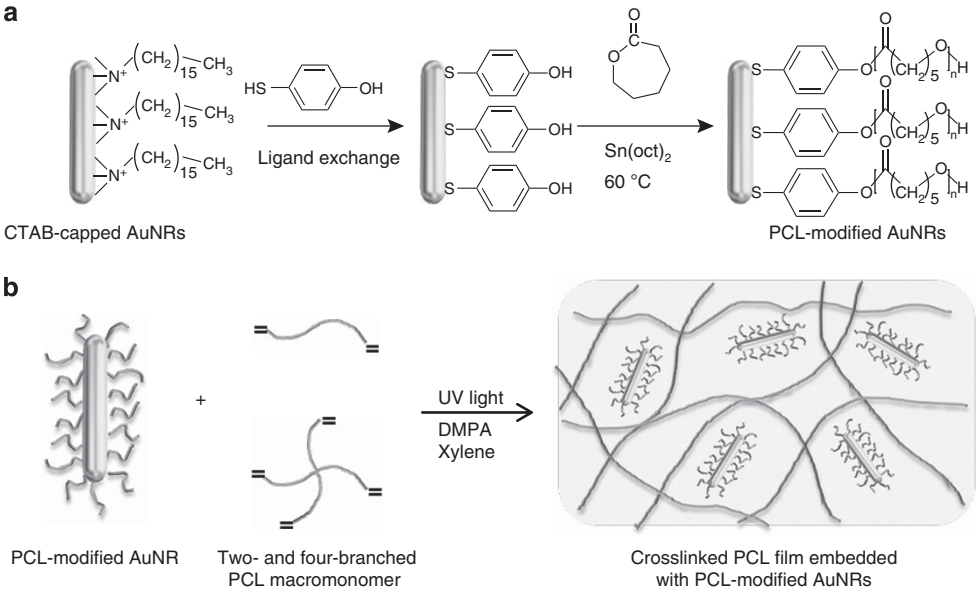

Figure 1 (**a**) Synthesis of poly(ε-caprolactone) (PCL)-modified gold nanorods (AuNRs) via surface-initiated ring-opening polymerization. (**b**) Preparation of AuNR-embedded PCL films through cross-linking of two- and four-branch PCL macromonomers in the presence of PCL-modified AuNRs. A full color version of this figure is available at *Polymer Journal* online.

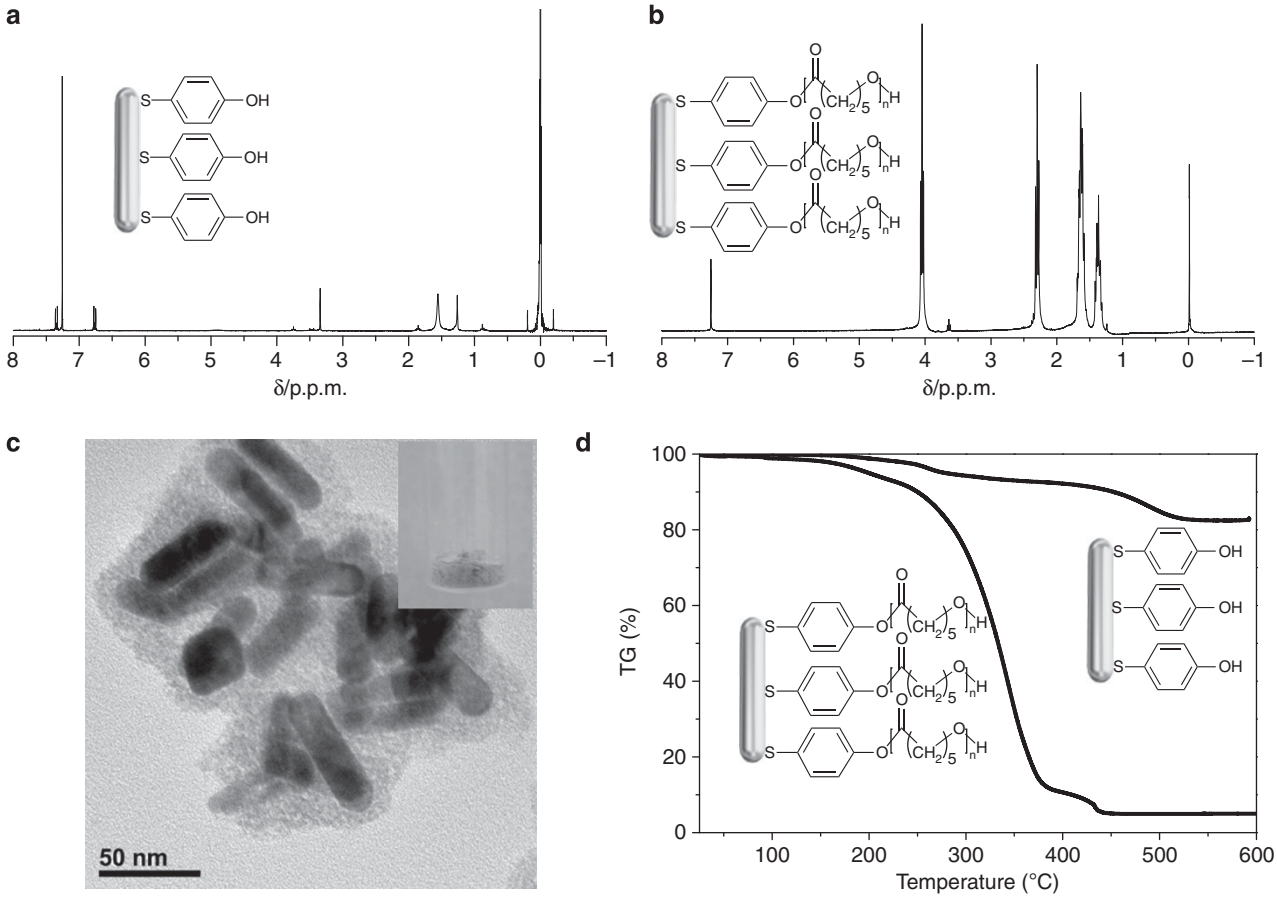

Figure 2 Characterizations of the poly(ε-caprolactone) (PCL)-modified gold nanorods (AuNRs). ^{1}HNMR spectra of AuNRs after (**a**) a ligand-exchange reaction with 4-mercaptophenol and (**b**) modification with PCL. (**c**) A transmission electron microscopy (TEM) image of PCL-modified AuNRs. The inset image shows PCL-modified AuNRs. (**d**) The thermogravimetric-differential thermal analysis (TG-DTA) curves for AuNRs after a ligand-exchange reaction with 4-mercaptophenol and modification with PCL. A full color version of this figure is available at *Polymer Journal* online.

constant beam diameter of 5.6 mm. The surface temperatures of the film samples were measured using an infrared thermal imaging camera during the irradiation with NIR light.

RESULTS AND DISCUSSION

Figure 1 shows the procedure to synthesize gold nanorod-embedded PCL films. In this study, to adjust the shape-memory-switching temperatures to values near-body temperature, two- and four-branched PCL macromonomers with acryloyl terminal group were cross-linked according to our previous work.[24] In general, incorporating rigid segments or blending with other components are the most studied methods to decrease the T_m of PCL.[1,25] However, the incorporation of non-PCL components usually hinders the crystallization and diminishes the melting enthalpies (ΔH_m). Therefore, we adjusted the T_m of PCL by tailoring the nanoarchitectures of the PCL macromonomers in this study.

We prepared two different films with 50/50 and 70/30 wt% of 2b- and 4b-PCL macromonomers. The films were fabricated via the photo-initiated polymerization of the PCL macromonomers in xylene in the presence of AuNRs. AuNRs are usually produced by the simple seed-mediated approach, and CTAB is used as a surfactant to produce a high yield of monodisperse nanorods.[26] Because the stability of the CTAB-capped AuNRs is known to be poor in nonpolar solvents and because the irreversible aggregation of AuNRs occurs in xylene, the surfaces of the AuNRs were also modified with PCL using the 'grafting from' method to incorporate the nanorods homogenously within the films (Figure 2a). First, hydroxyl groups were introduced onto the surface of the AuNRs to replace CTAB by mixing 4-mercaptophenol and AuNRs in THF. Then, PCL was grown on the surface of AuNRs using SI-ROP. Figure 2a shows the ^{1}HNMR spectra of AuNRs decorated with 4-mercaptophenol. By comparing the integral area of the terminal methyl of the alkyl chain ($\delta = 0.88$) and the protons in the benzene ring ($\delta = 7.33$, 7.36), approximately 66.7% of the CTAB was successfully exchanged with 4-mercaptophenol.

To characterize the molecular weight of the PCL grafted on the surface of AuNRs, iodine was used to cleave the Au–S covalent bonding. The molecular weight was calculated from the integration area of the methylene proton adjacent to the terminal hydroxyl group ($\delta = 3.64$) and the protons close to the ester bond (-$CH_2CH_2CH_2CH_2CH_2$O-, $\delta = 4.05$, italicized) (Figure 2b). A degree of polymerization of 41 was obtained. Figure 2c shows a TEM image of PCL-modified AuNRs. The average size of the AuNRs was 43.0 ± 3.7 nm (length) and 11.0 ± 1.0 nm (width), based on the TEM images. The visualization of the nanorods was achieved through negative staining with phosphotungstic aid, which was necessary because the polymer has insufficient electron density to be directly observed by TEM. The polymer appears as a light color layer surrounding the nanorods. The PCL-modified AuNRs shown in the

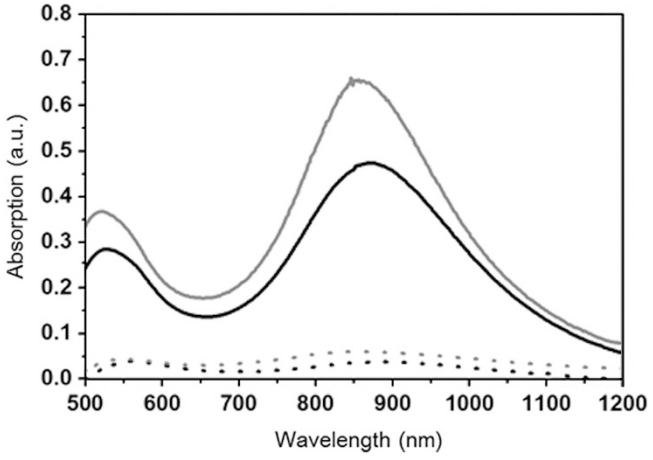

Figure 3 UV–Vis–NIR spectra of poly(ε-caprolactone) (PCL)-modified AuNRs embedded in 50/50 (black line) and 70/30 (gray line) PCL films with high (solid) and low (dotted) concentrations of nanorods.

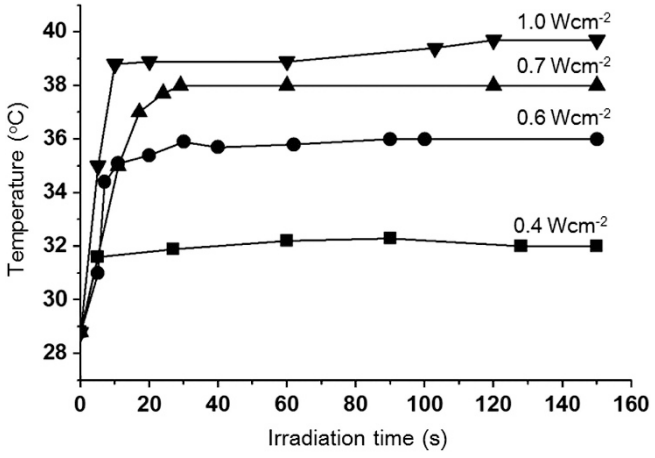

Figure 5 Heating profiles for 70/30 poly(ε-caprolactone) (PCL) films with 0.3 wt% of gold nanorods (AuNRs) under different near-infrared (NIR) laser intensities (805 nm); 0.4 (square), 0.6 (circle), 0.7 (triangle), 1.0 W cm^{-2} (inverted triangle).

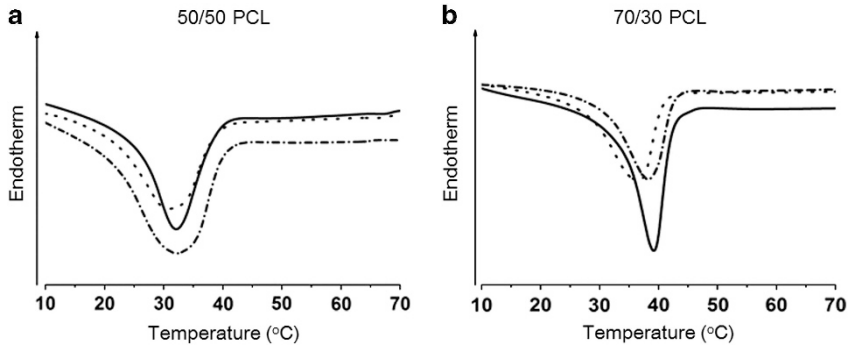

Figure 4 Differential scanning calorimeter (DSC) curves for (**a**) 50/50 and (**b**) 70/30 poly(ε-caprolactone) (PCL) films without (solid) and with high (solid) or low (dotted) concentrations of nanorods.

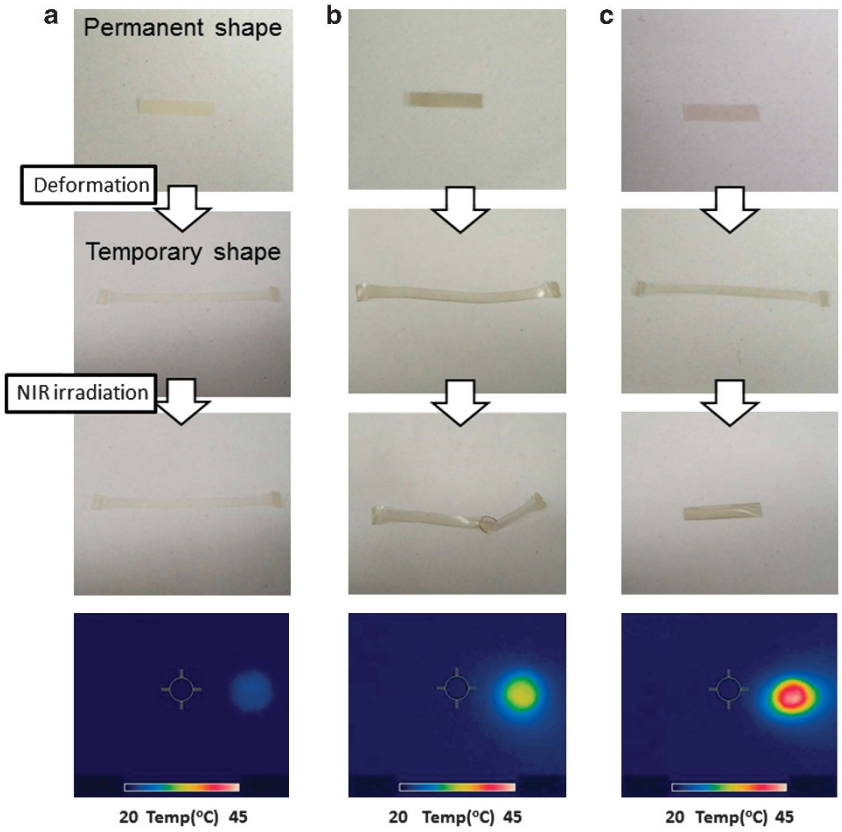

Figure 6 Images of the near-infrared (NIR) light-induced shape transitions of 70/30 poly(ε-caprolactone) (PCL) films with 0.3 wt% of gold nanorods (AuNRs). All the films were first heated to 40 °C (above T_m) and elongated to the predetermined strain of 100%. The temperature was then cooled to 4 °C (below T_c) for 10 min to fix the applied strain while preserving the tensile strain. The film without AuNRs were irradiated with 805-nm NIR at power density of 0.4 W cm^{-2} for a total of 10 s (**a**). The films with 0.3 wt% of AuNRs were irradiated with 805-nm NIR at power density of 0.4 W cm^{-2} (**b**) and 1 W cm^{-2} (**c**) for a total of 10 s of irradiation time. The infrared (IR) thermal images of the films after 10 s of NIR irradiation are also shown in the bottom images.

inset of (Figure 2c) have a homogeneous, slight pink color. The successful modification of the PCL on the nanorod surfaces was also confirmed by TGA (Figure 2d). It was found that below 200 °C, the weight loss of the PCL-modified AuNRs is 5%, while the weight loss of 4-mercaptophenol-modified AuNRs was approximately 1%, indicating that there is only limited water in both samples. Between 200 and 500 °C, the weight loss of PCL-modified AuNRs is 90%, while the weight loss of 4-mercaptophenol-modified AuNRs is 14%. Therefore, the successful surface modification of gold AuNRs by PCL was realized.

Next, we evaluated the effects of the surface modification on the stability or dispersity of AuNRs within the films. The dispersion of nanoparticles in polymer films has been an interesting topic, considering the significance of creating a homogenous nanocomposite.[27–30] UV–Vis–NIR spectroscopy is one of the best tools to monitor nanorod stability because the aggregation state of the nanorods affects their optical properties.[29,31] Due to the anisotropic shape of the nanorods, they display two separate SPR bands corresponding to their width and length, known as the transverse surface plasmon resonance (TSPR) and longitudinal surface plasmon resonance (LSPR), respectively. In general, a decrease in the peak absorption of LSPR can be observed when the particles aggregate. Supplementary Figure S1 in the supporting information shows the localized SPR absorption of freshly prepared CTAB-capped AuNRs in aqueous solution (solid line). Both TSPR and LSPR peaks can be clearly observed because the CTAB-capped AuNRs are well dispersed in aqueous solutions. A significant decrease in the LSPR is, however, observed for PCL-modified AuNRs in THF, which is a good solvent for PCL (dotted line). This behavior indicates an aggregation of AuNRs.

Figure 3 shows UV–Vis–NIR spectra of PCL-modified AuNRs embedded in PCL films. Both 50/50 and 70/30 PCL with the higher concentrations of nanorods (solid line) show strong peak adsorptions for TSPR and LSPR, although the peak adsorptions were not significant when the concentration of AuNRs was low (dotted line). This behavior indicates that AuNRs were uniformly embedded in the PCL films. When unmodified AuNRs were used, only one peak in the visible region was obtained (solid line in Supplementary Figure S2 in the supporting information). These results clearly indicate that the surface modification of the AuNRs with PCL is important for improving the stability of the particles within the PCL film.

In addition, the dispersity of the AuNRs within the films was studied using TEM. PCL 2b20 without acryloyl groups was mixed with PCL-modified AuNRs, and the image of a thin film composed of PCL 2b20 and PCL-AuNR (4 wt% and 0.16 wt% in xylene solution, respectively) is shown in Supplementary Figure S3 (in the supporting information). With the exception of a few aggregates (composed of several nanorods), most of the AuNRs can be dispersed well in PCL 2b20 thin films. This result agrees well with the evidence from the UV–Vis–NIR spectroscopy. To the best of our knowledge, several

factors, such as the molecular weights of the polymers grafted on the nanorod surfaces and the molecular weight of matrix polymer, would influence the miscibility of AuNRs.[27] Additionally, the varying curvature with the aspect ratios of the AuNRs makes the properties more interesting and complex.[32] A systematic study of the miscibility between the two components from a morphological viewpoint will be attempted in the future.

The thermal properties of PCL are also important from both a fundamental and technological perspective. In this study, we prepared cross-linked PCL films with two different T_m by optimizing the mixing ratios of the 2b- and 4b-PCL macromonomers. According to our previous report, increasing the 4b-PCL content leads to a near linear decrease in T_m and endothermic enthalpy change.[24] In Figures 4a and b, the cross-linked PCL films with 2b/4b ratios of 50/50 and 70/30 show a sharp transition over the T_m from approximately 30–33 and 37–40 °C, respectively. The degrees of crystallinity of all of the samples are listed in Supplementary Table S1 (in the supporting information). Importantly, the transition temperature did not change very much after the incorporation of the AuNRs. This observation is different from other reports. In general, nanoparticle incorporation results in the loss of crystallinity and a reduction in T_m.[19] It is plausible that the surface modification of the nanorods with PCL contributed to the prevention of the loss of crystallization in the PCL films.

To examine the heating potential of the films, samples were held within a beam of NIR light (805 nm). Figure 5 depicts a temperature increase with time for the 70/30 PCL film with 0.3 wt% (low concentration) of AuNRs under different laser intensities. The samples showed a sharp increase in the temperature during the first 10 s of irradiation before reaching a plateau. Higher intensity irradiation (1.0 W cm^{-2}) results in a higher final equilibrium temperature ($T = 39.7$ °C) compared with that attained with a lower excitation intensity (0.4 W cm^{-2}, $T = 32.0$ °C). Essentially, only small changes in temperature were observed for the samples that did not contain AuNRs (data not shown). These results indicate precise control over the sample heating through changes in the light intensity. The AuNR concentration also affects the heating profiles. However, we chose the lower concentration (0.3 wt%) of AuNRs for the following shape-memory experiments because this heat dissipation should be capable of producing rapid and complete shape-memory transformations in the physiological temperature range.

Finally, we examined the NIR light-induced shape-memory effect using a 70/30 PCL film with 0.3 wt% of AuNRs. The films were first heated to 40 °C (above T_m) and elongated to the predetermined strain of 100%. The temperature was then cooled to 4 °C (below T_c) for 10 min to fix the applied strain while preserving the tensile strain. The films were irradiated with 805-nm NIR at power densities of 0.4 and 1 W cm^{-2}, for a total of 10 s of irradiation time (Figure 6). The bottom images in Figure 6 show the IR thermal images of the films after 10 s irradiation. PCL films without AuNRs showed negligible recovery because the polymer absorbs minimally at the excitation wavelength (Figure 6a). When a beam with a power density of 0.4 W cm^{-2} impinged on an area of the PCL film with AuNRs, a shape change in the corresponding area was observed (Figure 6b). The IR thermal image also shows a temperature increase in the corresponding area.

The shape-memory transition was induced even though the observed temperature of the irradiated area was approximately 32 °C, which is lower than T_m. This result occurs because the thermal camera measures IR radiation from objects and estimates the surface temperatures. Therefore, the temperature inside the film could be higher than T_m. When exposed to 1 W cm^{-2} of NIR light, the film heated quickly to near-40 °C and changed back to its permanent, rectangular shape due to the heat dissipation to the entire film (Figure 6c). These results show the ability of the embedded AuNRs to heat a PCL film above its T_m and the spatial control of the shape in the physiological temperature range. We believe that this new remote NIR light-responsive PCL film may be a promising candidate for diverse applications, especially biomaterial development and basic cell biology.

CONCLUSIONS

In summary, NIR light-responsive shape-memory films were successfully prepared through the cross-linking of PCL macromonomers in the presence of AuNRs. First, the surface of AuNRs was modified with PCL through SI-ROP. This enabled the uniform incorporation of AuNRs into PCL film without hindering the crystallization of PCL. The shape-switching temperature was also adjusted in the physiological temperature range by controlling the melting temperature of PCL. Exposure to NIR light could successfully induce the photothermal heating of embedded AuNRs and, consequently, the shape-switching transition. Upon NIR irradiation, the film completely recovered its original shape. Local shape-memory transformation was also obtained when the limited area was exposed to light. These results show the potential ability of the AuNRs embedded PCL film as a remote and spatial controllable shape-memory material that actuates in physiologically relevant temperature ranges. This material is highly attractive for a wide range of applications, including safe and efficient transdermal SMP activation.

ACKNOWLEDGEMENTS

We express our gratitude to the Grant-in-Aid for Challenging Exploratory Research (23651142) from the Ministry of Education, Culture, Sports, Science and Technology (MEXT), Japan. This research is also partially funded by the Japan Society for the Promotion of Science (JSPS) through the 'Funding Program for World-Leading Innovative R&D on Science and Technology (FIRST Program),' initiated by the Council for Science and Technology Policy (CSTP).

1 Lendlein, A. & Langer, R. Biodegradable, elastic shape-memory polymers for potential biomedical applications. *Science* **296,** 1673–1676 (2002).
2 Lendlein, A. & Kelch, S. Shape-memory polymers. *Angew. Chem. Int. Ed.* **41,** 2034–2057 (2002).
3 Small, W., Singhal, P., Wilson, T. S. & Maitland, D. J. Biomedical applications of thermally activated shape memory polymers. *J. Mater. Chem.* **20,** 3356–3366 (2010).
4 Ebara, M., Uto, K., Idota, N., Hoffman, J. M. & Aoyagi, T. Shape-memory surface with dynamically tunable nano-geometry activated by body heat. *Adv. Mater.* **24,** 273–278 (2012).
5 Kweon, H., Yoo, M. K., Park, I. K., Kim, T. H., Lee, H. C., Lee, H. S., Oh, J. S., Akaike, T. & Cho, C. S. A novel degradable polycaprolactone networks for tissue engineering. *Biomaterials* **24,** 801–808 (2003).
6 Lendlein, A., Schmidt, A. M. & Langer, R. AB-polymer networks based on oligo(epsilon-caprolactone) segments showing shape-memory properties. *Proc. Natl Acad. Sci. USA* **98,** 842–847 (2001).
7 Rodriguez, E. D., Luo, X. F. & Mather, P. T. Linear/network poly(epsilon-caprolactone) blends exhibiting shape memory assisted self-healing (SMASH). *ACS Appl. Mat. Interfaces* **3,** 152–161 (2011).
8 Neuss, S., Blomenkamp, I., Stainforth, R., Boltersdorf, D., Jansen, M., Butz, N., Perez-Bouza, A. & Knuchel, R. The use of a shape-memory poly(epsilon of-caprolactone)dimethacrylate network as a tissue engineering scaffold. *Biomaterials* **30,** 1697–1705 (2009).
9 Ebara, M., Uto, K., Idota, N., Hoffman, J. M. & Aoyagi, T. The taming of the cell, shape-memory nanopatterns direct cell orientation. *Int. J. Nanomed.* doi: http://dx.doi.org/10.2147/IJN.S50677 (in press).
10 Ebara, M., Uto, K., Idota, N., Hoffman, J. M. & Aoyagi, T. Rewritable and shape-memory soft matter with dynamically tunable microchannel geometry in a biological temperature range. *Soft Matter* **9,** 3074–3080 (2013).

11 Jain, P. K., Huang, X. H., El-Sayed, I. H. & El-Sayed, M. A. Noble metals on the nanoscale: optical and photothermal properties and some applications in imaging, sensing, biology, and medicine. *Acc. Chem. Res.* **41,** 1578–1586 (2008).
12 Duchowicz, R., Scaffardi, L. B., Costela, A., Garcia-Moreno, I., Sastre, R. & Acuna, A. U. Photothermal analysis of polymeric dye laser materials excited at different pump rates. *Appl. Opt.* **42,** 1029–1035 (2003).
13 Loarer, T., Greffet, J. J. & Huetzaubert, M. Noncontact surface-temperature measurement by means of a modulated photothermal effect. *Appl. Opt.* **29,** 979–987 (1990).
14 Giljohann, D. A., Seferos, D. S., Daniel, W. L., Massich, M. D., Patel, P. C. & Mirkin, C. A. Gold nanoparticles for biology and medicine. *Angew. Chem. Int. Ed.* **49,** 3280–3294 (2010).
15 Huang, X. H., Jain, P. K., El-Sayed, I. H. & El-Sayed, M. A. Plasmonic photothermal therapy (PPTT) using gold nanoparticles. *Lasers Med. Sci.* **23,** 217–228 (2008).
16 Huang, X. H., El-Sayed, I. H., Qian, W. & El-Sayed, M. A. Cancer cell imaging and photothermal therapy in the near-infrared region by using gold nanorods. *J. Am. Chem. Soc.* **128,** 2115–2120 (2006).
17 Weissleder, R. A clearer vision for *in vivo* imaging. *Nat. Biotechnol.* **19,** 316–317 (2001).
18 Hribar, K. C., Metter, R. B., Ifkovits, J. L., Troxler, T. & Burdick, J. A. Light-Induced temperature transitions in biodegradable polymer and nanorod composites. *Small* **5,** 1830–1834 (2009).
19 Le, D. M., Tycon, M. A., Fecko, C. J. & Ashby, V. S. Near-infrared activation of semi-crystalline shape memory polymer nanocomposites. *J. Appl. Polym. Sci.* **130,** 4551–4557 (2013).
20 Li, Y. N., Yu, D. S., Dai, L. M., Urbas, A. & Li, Q. A. Organo-soluble chiral thiol-monolayer-protected gold nanorods. *Langmuir* **27,** 98–103 (2011).
21 Pitt, C. G., Jeffcoat, A. R., Zweidinger, R. A. & Schindler, A. Sustained drug delivery systems. I. The permeability of poly(epsilon-caprolactone), poly(DL-lactic acid), and their copolymers. *J. Biomed. Mater. Res.* **13,** 497–507 (1979).
22 Nikoobakht, B. & El-Sayed, M. A. Preparation and growth mechanism of gold nanorods (NRs) using seed-mediated growth method. *Chem. Mater.* **15,** 1957–1962 (2003).
23 Khanal, B. P. & Zubarev, E. R. Rings of nanorods. *Angew. Chem. Int. Ed.* **46,** 2195–2198 (2007).
24 Uto, K., Yamamoto, K., Hirase, S. & Aoyagi, T. Temperature-responsive cross-linked poly(ε-caprolactone) membrane that functions near body temperature. *J. Controlled Release* **110,** 408–413 (2006).
25 Jeong, H. M., Kim, B. K. & Choi, Y. J. Synthesis and properties of thermotropic liquid crystalline polyurethane elastomers. *Polymer* **41,** 1849–1855 (2000).
26 Lohse, S. E. & Murphy, C. J. The quest for shape control: a history of gold nanorod synthesis. *Chem. Mater.* **25,** 1250–1261 (2013).
27 Corbierre, M. K., Cameron, N. S., Sutton, M., Laaziri, K. & Lennox, R. B. Gold nanoparticle/polymer nanocomposites: dispersion of nanoparticles as a function of capping agent molecular weight and grafting density. *Langmuir* **21,** 6063–6072 (2005).
28 Hong, Z. K., Zhang, P. B., Liu, A. X., Chen, L., Chen, X. S. & Jing, X. B. Composites of poly(lactide-co-glycolide) and the surface modified carbonated hydroxyapatite nanoparticles. *J. Biomed. Mater. Res. Part A* **81A,** 515–522 (2007).
29 Heo, K., Miesch, C., Emrick, T. & Hayward, R. C. Thermally reversible aggregation of gold nanoparticles in polymer nanocomposites through hydrogen bonding. *Nano Lett.* **13,** 5297–5302 (2013).
30 Hore, M. J. A. & Composto, R. J. Using miscible polymer blends to control depletion-attraction forces between au nanorods in nanocomposite films. *Macromolecules* **45,** 6078–6086 (2012).
31 Corbierre, M. K., Cameron, N. S., Sutton, M., Mochrie, S. G. J., Lurio, L. B., Ruhm, A. & Lennox, R. B. Polymer-stabilized gold nanoparticles and their incorporation into polymer matrices. *J. Am. Chem. Soc.* **123,** 10411–10412 (2001).
32 Liu, H., Zhu, Y. L., Zhang, J., Lu, Z. Y. & Sun, Z. Y. Influence of grafting surface curvature on chain polydispersity and molecular weight in concave surface-initiated polymerization. *ACS Macro Lett.* **1,** 1249–1253 (2012).

Supplementary Information accompanies the paper on Polymer Journal website (http://www.nature.com/pj)